ACS Chemical Neuroscience

Research Article

pubs.acs.org/chemneuro

# Identification and Characterization of ML352: A Novel, Noncompetitive Inhibitor of the Presynaptic Choline Transporter

Elizabeth A. Ennis,[†] Jane Wright,[†] Cassandra L. Retzlaff,[†] Owen B. McManus,[#] Zhinong Lin,[#] Xiaofang Huang,[#] Meng Wu,[#] Min Li,[#] J. Scott Daniels,[†,∥,⊥] Craig W. Lindsley,[†,‡,∥,⊥] Corey R. Hopkins,[†,‡,∥,⊥] and Randy D. Blakely*[,†,§]

[†]Departments of Pharmacology, [‡]Chemistry, and [§]Psychiatry, [∥]Center for Neuroscience Drug Discovery, [⊥]Specialized Center for Probe Development, Vanderbilt University Medical Center, Nashville, Tennessee 37232, United States

[#]Johns Hopkins University Ion Channel Center, Baltimore, Maryland 21205, United States

**ABSTRACT:** The high-affinity choline transporter (CHT) is the rate-limiting determinant of acetylcholine (ACh) synthesis, yet the transporter remains a largely undeveloped target for the detection and manipulation of synaptic cholinergic signaling. To expand CHT pharmacology, we pursued a high-throughput screen for novel CHT-targeted small molecules based on the electrogenic properties of transporter-mediated choline transport. In this effort, we identified five novel, structural classes of CHT-specific inhibitors. Chemical diversification and functional analysis of one of these classes identified ML352 as a high-affinity ($K_i$ = 92 nM) and selective CHT inhibitor. At concentrations that fully antagonized CHT in transfected cells and nerve terminal preparations, ML352 exhibited no inhibition of acetylcholinesterase (AChE) or cholineacetyltransferase (ChAT) and also lacked activity at dopamine, serotonin, and norepinephrine transporters, as well as many receptors and ion channels. ML352 exhibited noncompetitive choline uptake inhibition in intact cells and synaptosomes and reduced the apparent density of hemicholinium-3 (HC-3) binding sites in membrane assays, suggesting allosteric transporter interactions. Pharmacokinetic studies revealed limited *in vitro* metabolism and significant CNS penetration, with features predicting rapid clearance. ML352 represents a novel, potent, and specific tool for the manipulation of CHT, providing a possible platform for the development of cholinergic imaging and therapeutic agents.

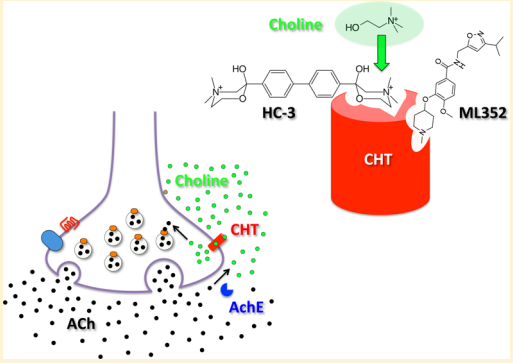


**KEYWORDS:** *Choline, acetylcholine, transport, hemicholinium-3, drug development*

The neurotransmitter acetylcholine (ACh) plays a critical role in autonomic function, motor control, attention, learning, and memory, and reward.[1−3] Consequently, multiple, devastating disorders have been linked to perturbations of cholinergic signaling, including Alzheimer's disease (AD),[4] Parkinson's disease (PD),[5] dystonia,[6,7] myasthenia,[8] schizophrenia,[9] and addiction,[10] among others. Cholinergic agents, including acetylcholinesterase inhibitors (AChEIs) and muscarinic/nicotinic receptor agonists and antagonists, are used to treat symptoms in diseases with either diminished or excessive cholinergic signaling, as in AD,[11] nicotine addiction,[12] and dystonia.[13] Although these agents have proven to be useful, their efficacy is reduced by dose-limiting side effects and, in some cases, a constitutive mode of cholinergic manipulation. Sustained synthesis of ACh is dependent on the efficient acquisition of choline by cholinergic terminals,[14] an activity exclusively mediated by the high-affinity choline transporter (CHT, *SLC5A7*).[15−18] Not surprisingly, full loss of CHT in transgenic mice produces a time-dependent elimination of cholinergic signaling that is incompatible with life.[19,20] Less radical genetic manipulations of CHT also result in significant biochemical, physiological, and behavioral effects, in keeping with a key contribution of the transporter to ACh signaling. Thus, CHT heterozygous animals exhibit reduced ACh levels and ACh release, basal and exercise-induced tachycardia,[21] and diminished neuromuscular signaling and motor endurance.[19] Elevated CHT expression leads to increased ACh levels and reduced motor fatigue.[22,23] With respect to CNS function, CHT heterozygous animals demonstrate reduced performance on tasks that require sustained attention in the presence of distraction[24] and in tests of behavioral flexibility[25] as well as diminished dopamine elevations following cocaine or nicotine challenge,[26] whereas CHT overexpressing mice exhibit anxiety/depression behaviors.[27] In keeping with these rodent studies, functional polymorphisms in the *SLC5A7* gene have been linked to neuromuscular disorders,[28] elevated distractibility[29] and ADHD,[30] and depression.[31]

CHT is conspicuous in being absent from current efforts to pharmacologically manipulate cholinergic function, but it may possess advantages in therapeutic targeting related to its activity-dependent support of cholinergic signaling,[32,33] mediated by a

**Received:** August 10, 2014
**Revised:** December 19, 2014
**Published:** January 5, 2015

  

DOI: 10.1021/cn5001809
*ACS Chem. Neurosci.* 2015, 6, 417−427

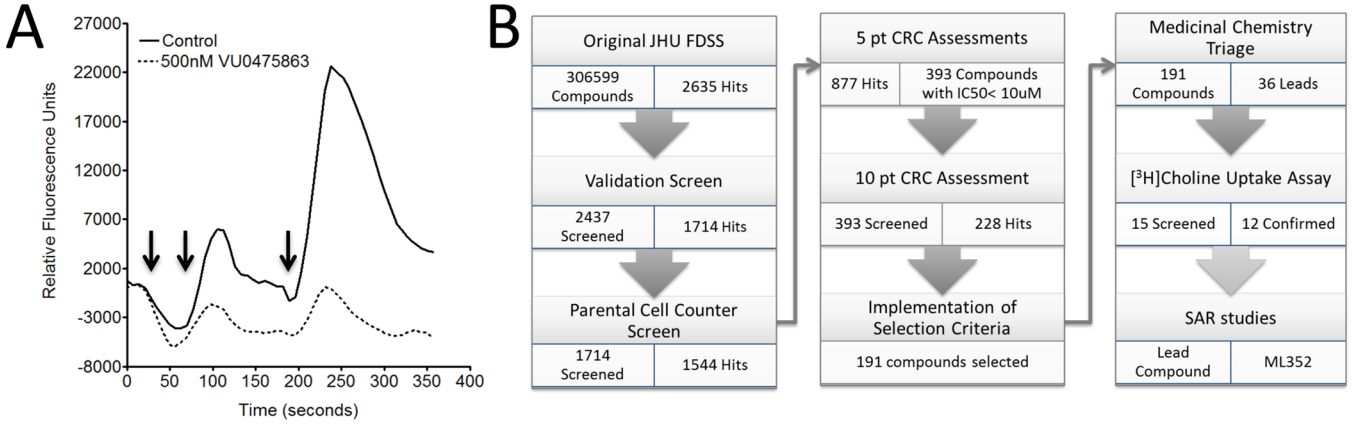


**Figure 1.** High-throughput screen for CHT inhibitors. (A) Example of screening assay. Triple-add protocol for screening library compounds for choline-induced membrane depolarization in HEK hCHT LV-AA cells. Time points for addition of vehicle, $EC_{20}$ choline (500 nM), and $EC_{80}$ (60 $\mu$M) choline are noted as arrows, left to right, respectively (solid line). Depolarization arising from three-add protocol in the presence of 500 nM VU0475863, one of the final 15 hit compounds and a progenitor of ML352, is show in overlay (dotted line). (B) Screening workflow. Shown is our progression through the 9 major phases of the screen with the respective number of compounds that entered (small left-hand boxes) and exited (small right-hand boxes) each phase.

steady-state enrichment on cholinergic synaptic vesicles, where it can move to the plasma membrane in response to cholinergic neuron activation.[24,34,35] This feature also suggests that CHT-targeted antagonists may display use-dependence, thereby limiting drug effects to states of intense cholinergic signaling. CHT-mediated choline transport can be effectively attenuated by the competitive antagonist hemicholinium-3 (HC-3).[36−38] Unfortunately, many of the properties of HC-3, including the presence of two choline-like quartenary nitrogens as well as its limited CNS penetrance and challenging chemical synthesis, restrict the use of the molecule as a tool for mechanistic studies or as a starting point for the development of imaging or therapeutic agents. However, in the more than 50 years since the first synthesis of HC-3,[39,40] no other widely utilized CHT-targeted agents have been developed. To expand CHT pharmacology, we took advantage of the electrogenic nature of CHT-supported choline uptake to implement a membrane potential-based, high-throughput screen for CHT modulators.[41,42]

Although CHT has been known to play a critical role in dictating cholinergic signaling capacity for many decades,[38,43,44] the transporter is conspicuously absent from targets engaged for the therapeutic manipulation of cholinergic signaling. In part, this may be due to the understanding that full elimination of transporter function in vertebrates, as seen with CHT knockout mice,[20] is incompatible with life. In CHT knockout mice, however, loss of CHT expression occurs throughout life, irrespective of demand, and thus the model may poorly represent the therapeutic limitations associated with CHT antagonism. Possibly, attenuated cholinergic signaling, rather than full inhibition, may offer an effective treatment for disorders where hypercholinergic function has been proposed as a major etiological component. For example, the uncontrolled movements associated with dystonia are commonly treated with anticholinergic agents to reduce both central and peripheral control of motor function.[13,45] Hypercholinergic function has also been associated with depression and anxiety behaviors.[46,47] In the latter case, the nonspecific muscarinic ACh receptor antagonist scopolamine has received significant attention as a rapidly acting antidepressant.[48,49] Finally, ACh receptor stimulation is intimately involved in the modulation of reward circuits, where anticholinergics have been shown to reduce aspects of reward signaling[50,51] and CHT heterozygous mice have been found to demonstrate reduced dopamine release in response to cocaine and nicotine.[26]

The importance of CHT in determining ACh signaling capacity, the therapeutic potential of CHT antagonism, and the limitations of HC-3 noted above encouraged us to pursue a high-throughput screen to identify novel CHT modulators. Here, we report the results of our screen for CHT inhibitors. We describe a novel, non-choline-based, CHT-targeted inhibitor (ML352) that demonstrates nanomolar CHT antagonism as well as selectivity for CHT in relation to multiple transporters, ion channels, and receptors. Our kinetic studies with ML352 are the first to demonstrate the possibility of allosteric modulation of the transporter and offer a novel path to the development of cholinergic therapeutics.

## RESULTS AND DISCUSSION

**High-Throughput Screen for CHT Antagonists.** To establish a screen for novel CHT inhibitors, we capitalized on the significantly elevated surface expression of the human transporter bearing alanine substitutions for two amino acids, L531 and V532, that constitute a strong dileucine-type endocytic sequence.[41] In addition to the greatly enhanced choline-activated membrane depolarization achieved in hCHT LV-AA cells, the removal of strong endocytic sequences lessens the possibility that compounds that reduce choline-induced membrane depolarization do so by triggering transporter endocytosis. Using these cells, we instituted a triple-add protocol that involved addition of vehicle or inhibitor in the absence of choline, followed 1 min later by the addition of an $EC_{20}$ concentration (500 nM) of choline, followed 2 min later by the addition of an $EC_{80}$ concentration (60 $\mu$M) of choline. To identify noncompetitive and potentially allosteric inhibitors distinct from HC-3, we focused on compounds that reduced signal at the $EC_{80}$ choline concentration, also capturing the superior signal/noise characteristics associated with signals generated at or near the CHT $V_{max}$. Figure 1A demonstrates the fluorescence emission from the triple-add protocol following addition of choline alone or choline in the presence of an inhibitor, a structural predecessor to the focus of this article, ML352.


DOI: 10.1021/cn5001809
ACS Chem. Neurosci. 2015, 6, 417−427

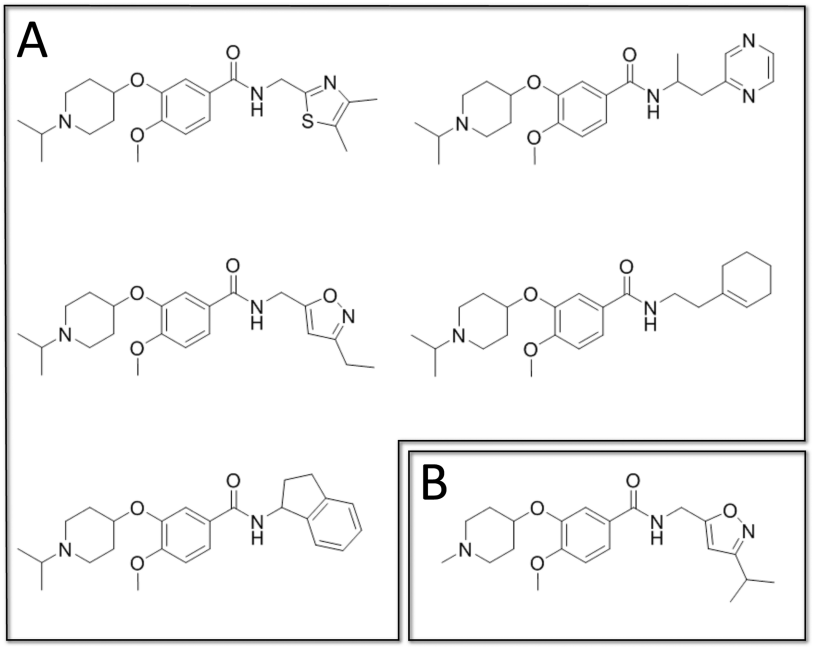


**Figure 2.** CHT inhibitor stuctures. (A) Structures of selected compounds derived as hits in the triple-add protocol based on repeated, dose-dependent inhibition of choline-induced membrane depolarization at $EC_{80}$ choline concentration by ≥50% at 10 $\mu$M inhibitor concentration. (B) Structure of ML352.

Using the triple-add format, we screened >300 000 compounds from the NIH Molecular Library Small Molecule Repository (MLSMR) compound collection (http://mli.nih.gov/mli/secondary-menu/mlscn/ml-small-molecule-repository/) at 60 $\mu$M, and, based on a cutoff criteria of 3 SD from the mean $EC_{80}$ choline-induced fluorescence, we identified 2635 preliminary hits, a 0.86% hit rate. We were able to validate CHT depolarization inhibition by 1714 of these compounds available for retesting, an ∼65% replication rate. These compounds were then tested in a counterscreen against nontransfected HEK 293 cells, where we found that 90% of these compounds lacked CHT-independent depolarization-inducing activity, yielding 1544 molecules for further analysis. Next, 5-point concentration response curves (CRC) were performed using the hCHT LV-AA based membrane depolarization assay. In this effort, we found that 57%, or 877, of the compounds displayed dose-dependent inhibitory activity. From this group, we selected 393 molecules based on having $IC_{50}$ values lower than 10 $\mu$M to more carefully analyze in 10-point CRC assays, which yielded 228 molecules that retained high potency for inhibition of choline-induced depolarization. Of these compounds, 191 displayed no inherit fluorescence and retained their $EC_{80}$ inhibitory potency upon repeat testing. Inspection of the molecules in this group revealed 5 major structural classes, comprising 36 molecules, whose structures also indicated suitability for chemical modifications and *in vivo* use. As membrane depolarization that arises with CHT activity is nonstoichiometrically linked to choline flux,[42] we next selected 15 molecules derived from 3 of these classes for 5-point CRC tests, now targeting inhibition of [$^3$H]choline uptake, again using hCHT LV-AA cells. In the latter tests, 12 molecules demonstrated significant, dose-dependent inhibitory activity, 5 of which belong to the one class selected for chemical diversification (Figure 2A). Details of our chemical diversification efforts will be described elsewhere. In this effort, we produced VU0476328 *N*-((3-isopropylisoxazol-5-yl)methyl)-4-methoxy-3-((1-methylpiperidin-4-yl)oxy)benzamide (Figure 2B; hereafter designated ML352) as our most potent derivative and describe its characterization below.

**Potency and Specificity of ML352.** First, we sought to confirm the potency and specificity of ML352 for inhibition of hCHT LV-AA in transfected HEK 293 cells. In these studies (Figure 3A), we found that ML352 inhibited [$^3$H]choline uptake with high affinity ($K_i = 92 \pm 2.8$ nM), with data well-fit to a single-site inhibition model ($r = 0.935$) In Figure 4B, we demonstrate that ML352 choline uptake inhibition was retained when tested in mouse forebrain synaptosomes ($K_i = 166 \pm 12$ nM). We also observed a lack of inhibitory activity at the dopamine transporter (DAT), the norepinephrine transporter (NET), and the serotonin transporter (SERT) in transfected HEK 293 cells as well as an insensitivity of [$^3$H]choline accumulation in nontransfected HEK 293 cells to ML352 (<20% at 5 $\mu$M, data not shown). Regardless, these assays rule out a nonspecific effect on membrane integrity or alterations of ion gradients as being the basis for CHT inhibition. Additionally, little or no activity (>50% inhibition at 10 $\mu$M) was detected against 68 G-protein-coupled receptors (GPCRs), ion channels, and transporters in the EuroFin Lead Profiling Screen (Table 1), highlighting a clean ancillary pharmacology profile. The lack of choline and HC-3-mimicking quartenary nitrogens in the progenitor of ML352 suggested the possibility of limited interactions with other proteins that recognize choline or ACh. Indeed, in brain preparations, we also found no ability of ML352 to inhibit the biosynthetic enzyme ChAT and the metabolizing enzyme AChE at concentrations of ML352 well above the CHT $K_i$ (Figure 3C,D). Evaluation of ML352 and its future derivatives for interactions with other targets is, of course, incomplete, and more extensive evaluations, both *in vitro* and *in vivo*, will continue to be pursued, as should studies using these agents to manipulate cholinergic physiology and behavior.

**Kinetic Mode of ML352 Antagonism of CHT.** To establish a mechanism for CHT antagonism by ML352 and to classify the


DOI: 10.1021/cn5001809
*ACS Chem. Neurosci.* 2015, 6, 417−427

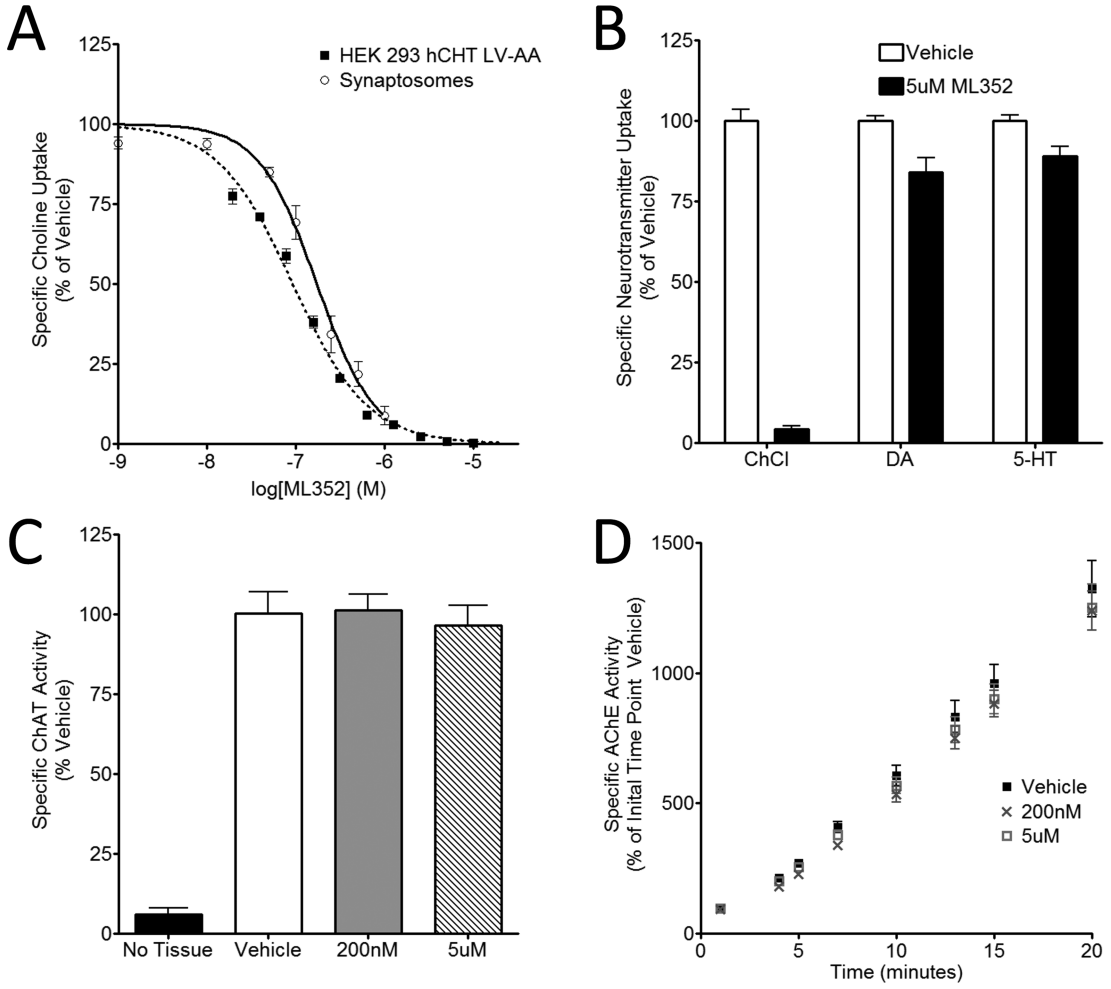


**Figure 3.** Functional evaluation of ML352. (A) Inhibition of choline transport by ML352 in HEK 293 cells transfected with hCHT LV-AA cells and mouse forebrain synaptosomes. ML352 inhibited choline uptake with $K_i = 92 \pm 2.8$ nM ($n = 3$) and in mouse forebrain synaptosomes with $K_i = 172 \pm 12$ nM ($n = 3$). (B) ML352 at 5 $\mu$M fails to inhibit DAT and SERT in mouse forebrain synaptosomes ($n = 3$). (C) ML352 lacks activity for inhibition of ChAT activity in mouse forebrain extracts ($n = 3$). (D) ML352 lacks activity for inhibition of AChE in mouse forebrain extracts ($n = 3$).

molecule as similar to or distinct from HC-3 in action, we pursued studies of the kinetic basis of ML352 antagonism of choline transport activity (Figure 4A,B). In studies examining the activity of the inhibitor at varying concentrations of choline in transport assays with hCHT LV-AA transfected cells, we observed saturable choline transport with a $K_m$ for choline of $2.5 \pm 0.4$ $\mu$M, consistent with prior reports[52] (Figure 4A). When combined with fixed concentrations of ML352, we observed no significant effect on the choline $K_m$ (200 nm ML352, $K_m = 4.4 \pm 1.2$ $\mu$M; 800 nM, $K_m = 4.4 \pm 2.0$ $\mu$M), whereas a concentration-dependent reduction in transport $V_{max}$ relative to vehicle-treated control was evident ($V_{max}$ 200 nM ML352 = 70.4 ± 5.6%; 800 nM, 30.3 ± 4.2%). Analysis of ML352 inhibitory actions on choline uptake in mouse forebrain synaptosomes yielded similar effects ($V_{max}$ 300 nM ML352 = 57.2 ± 3.4%) (Figure 4B). Together, these findings are consistent with the potent antagonism of CHT-dependent membrane potential of ML352 precursors when tested at the $EC_{80}$ choline concentration and point to a noncompetitive mode of CHT inhibition, distinct from the competitive mode of inhibition shown by HC-3.[53,54] A noncompetitive mechanism is a potentially useful feature of ML352 inhibition in that extracellular choline has been reported at near saturating levels in brain extracellular fluid,[55] and much higher concentrations of competitive antagonists, like HC-3, might be needed to effect CHT antagonism *in vivo*, leading to off-target actions.

HC-3 is the sole CHT antagonist in common use, and is limited essentially to mechanistic studies of cholinergic signaling.[56] Developed in the late 1950s by Schueler and colleagues,[39] HC-3 is a bicyclic compound with two quartenary nitrogens that mimics choline's structure. The latter property affords orthosteric, high-affinity interactions with CHT. The choline features of HC-3, however, also provide for interactions with other choline targets such as CTL1-type choline transporters involved in choline lipid biosynthesis[57] and choline kinase,[58] with curvilinear binding kinetics reflecting multisite and/or cooperative binding interactions further limiting its use.[59] With respect to *in vivo* utility, constitutive positive charge of HC-3 impedes CNS penetration and thus limits the molecule's use in the potential treatment of brain disorders or in imaging CNS cholinergic innervation.[60] Whereas HC-3 has proven to be useful in documenting CHT density in both membrane binding assays[61] and autoradiographic studies,[62] PET studies that document cholinergic neuron projections and/or terminals are currently limited, with a primary focus on derivatives of the vesicular choline transporter antagonist vesamicol.[63] Depending on access of novel CHT ligands to intracellular versus extracellular conformations, targeting CHT may afford labeling


DOI: 10.1021/cn5001809
*ACS Chem. Neurosci.* 2015, 6, 417−427

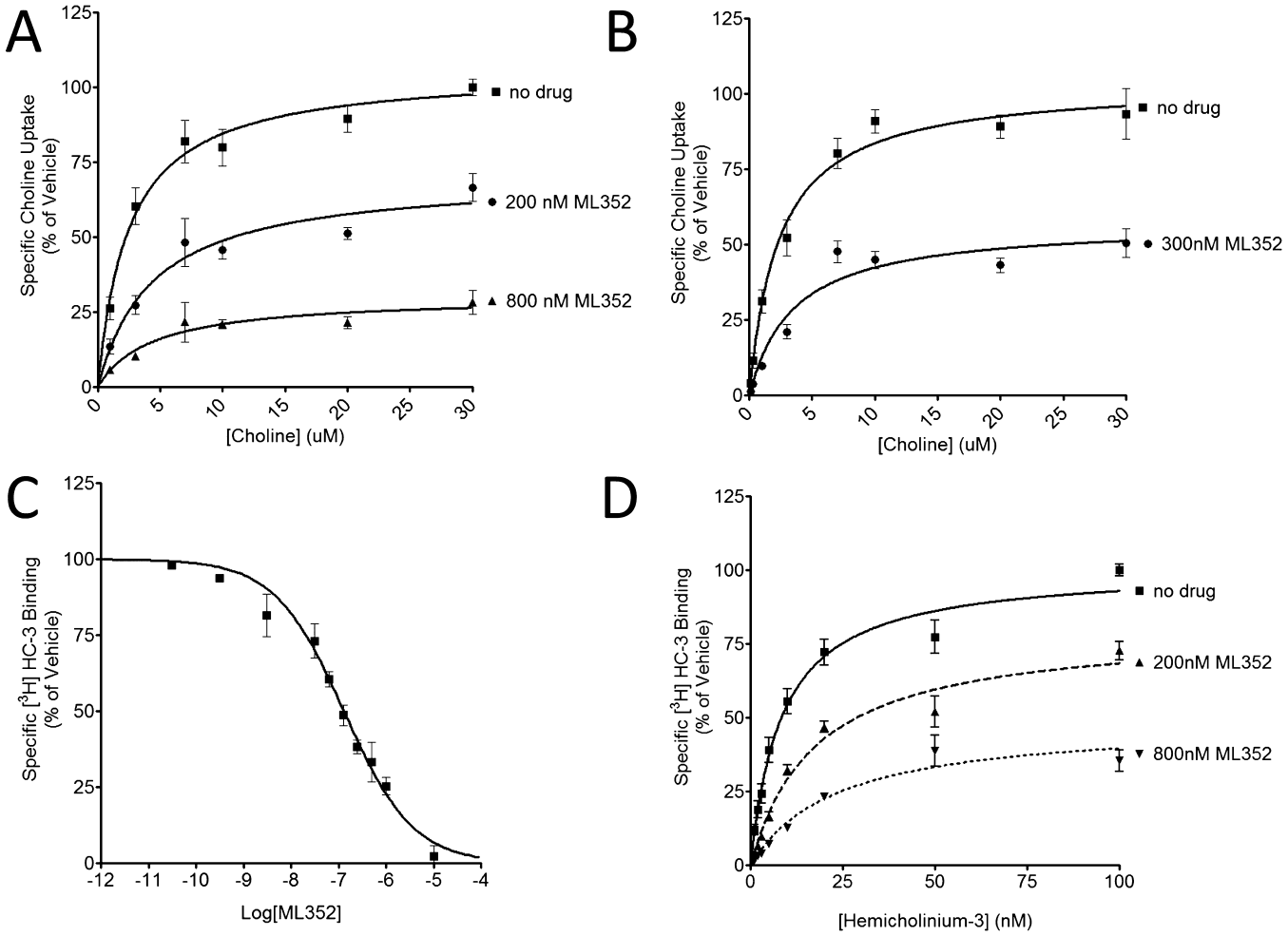


**Figure 4.** Inhibitory mechanisms involved with ML352 antagonism of CHT. (A) ML352 noncompetitively inhibits choline uptake in hCHT LV-AA cells. Inclusion of ML352 at 200 or 800 nM in saturation choline transport assays reveals a progressive decrease in the choline transport $V_{max}$ without changing choline $K_m$ ($n = 3$). (B) ML352 noncompetitively inhibits choline uptake in mouse forebrain synaptosomes. Inclusion of ML352 at 300 nM in saturation choline transport assays reveals a decrease in the choline transport $V_{max}$ without a change in choline $K_m$ ($n = 3$). (C) Inhibition of [$^3$H]HC-3 binding to transfected cell membranes by ML352. Binding assays revealed a ML352 $K_i$ of 128.6 ± 15.3 nM ($n = 3$). (D) ML352 exhibits noncompetitive inhibition of [$^3$H]HC-3 binding to transfected cell membranes. Increasing concentrations of [$^3$H]HC-3 ± 200 nM ML352 yielded a significant reduction in binding $B_{max}$ with no change in [$^3$H]HC-3 $K_d$. At 800 nM ML352, a further reduction in $B_{max}$ was detected along with an increase in [$^3$H]HC-3 $K_d$ ($n = 4$).

of activated cholinergic neurons where synaptic CHT density is elevated relative to less active states.[24,34,35]

To assess whether the binding site occupied by ML352 is kinetically independent of that occupied by HC-3, we pursued [$^3$H]HC-3 binding inhibition studies using membranes from HEK hCHT cells (Figure 4C,D). First, we observed that ML352 demonstrated dose-dependent inhibition of HC-3 binding, well-fit by a single-site inhibition model ($r = 0.948$) with a $K_i$ of 128.6 ± 15.3 nM (Figure 4C), similar to that found in uptake inhibition studies. Next, we performed saturation binding studies using [$^3$H]HC-3, observing good ($r = 0.93$), single-site fit to binding data with a $K_d$ of 8.5 ± 1.1 nM (Figure 4D), similar to previous observations.[53] In support of uptake inhibition findings, we observed a significant reductions in [$^3$H]HC-3 binding $B_{max}$ ($B_{max}$ 200 nM ML352 = 80.3 ± 3.8%; 800 nM, 48.9 ± 4.1%). ML352 had no significant effect on [$^3$H]HC-3 $K_d$ at 200 nM (17.4 ± 2.3), whereas an increased $K_d$ was detected at 800 nM (23.4± 5.0). [$^3$H]HC-3 binding with mouse and rat brain membranes exhibited multisite binding kinetics, as previously described,[59] precluding accurate assessment of kinetic parameters in native tissues. Nontheless, our studies provide strong support for the idea that choline uptake inhibition by ML352 is due to drug interactions at a site distinct from that occupied by either the substrate or HC-3.

**ML352 Modulation of CHT Surface Expression.** Recently, HC-3 was reported to induce elevated surface expression of CHT.[64] To determine whether this property is shared by ML352, we performed cell-surface biotinylation studies, testing ML352 after 15 min incubations, in parallel with vehicle, HC-3, or choline treated cells. We used HEK 293 cells stably transfected with WT CHT for these studies, as the hCHT LV-AA mutant carries a compromised trafficking sequence that could obscure drug-induced changes in cell-surface expression. As shown in Figure 5, we replicated the findings that HC-3 elevates steady-state CHT surface expression (76 ± 16% of control), although we obtained no evidence for the previously reported choline-dependent reductions.[64] ML352 at saturating concentrations (5 μM) also induced a significant increase in hCHT surface expression (43.4 ± 4.7% of control). No impact of drugs was seen on total CHT protein expression


DOI: 10.1021/cn5001809
ACS Chem. Neurosci. 2015, 6, 417−427

**Table 1. Off-Target Interactions of ML352**

| target | % inhibition[a] | target | % inhibition[a] |
|---|---|---|---|
| Adenosine $A_1$ | −5 | Histamine, $H_3$ | 7 |
| Adenosine $A_{2A}$ | 0 | Imidazoline $I_2$, Central | 16 |
| Adenosine $A_3$ | 4 | Interleukin IL-1 | −2 |
| Adrenergic $\alpha_{1A}$ | 23 | Leukotriene, Cysteinyl $CysLT_1$ | −3 |
| Adrenergic $\alpha_{1B}$ | 3 | Melatonin $MT_1$ | 5 |
| Adrenergic $\alpha_{1D}$ | 24 | Muscarinic $M_1$ | 32 |
| Adrenergic $\alpha_{2A}$ | 43 | Muscarinic $M_2$ | 12 |
| Adrenergic $\beta_1$ | 2 | Muscarinic $M_3$ | 26 |
| Adrenergic $\beta_2$ | 43 | Neuropeptide Y $Y_1$ | −2 |
| Androgen (Testosterone) AR | 8 | Neuropeptide Y $Y_2$ | 7 |
| Bradykinin $B_1$ | 6 | Nicotinic Acetylcholine | 13 |
| Bradykinin $B_2$ | −3 | Nicotinic Acetylcholine $\alpha$1, Bungarotoxin | 7 |
| Calcium Channel L-Type, Benzothiazepine | 3 | Opiate $\delta_1$ (OP1, DOP) | −2 |
| Calcium Channel L-Type, Dihydropyridine | 13 | Opiate $\kappa$ (OP2, KOP) | 22 |
| Calcium Channel N-Type | −1 | Opiate $\mu$ (OP3, MOP) | 8 |
| Cannabinoid $CB_1$ | 4 | Phorbol Ester | 5 |
| Dopamine $D_1$ | 9 | Platelet Activating Factor (PAF) | −4 |
| Dopamine $D_{28}$ | 18 | Potassium Channel [$K_{ATP}$] | 4 |
| Dopamine $D_3$ | 15 | Potassium Channel hERG | 16 |
| Dopamine $D_{42}$ | −3 | Prostanoid $EP_4$ | −7 |
| Endothelin $ET_A$ | −3 | Purinergic P2X | 22 |
| Endothelin $ET_B$ | −2 | Purinergic P2Y | 19 |
| Epidermal Growth Factor (EGF) | 5 | Rolipram | 1 |
| Estrogen Er$\alpha$ | 4 | Sertonin (5-Hydroxytrptamine) 5-$HT_{1A}$ | 40 |
| $GABA_A$, Flunitrazepam, Central | 6 | Sertonin (5-Hydroxytrptamine) 5-$HT_{2B}$ | −7 |
| $GABA_A$, Muscimol, Central | 9 | Sertonin (5-Hydroxytrptamine) 5-$HT_3$ | 2 |
| $GABA_{B1A}$ | −9 | Sigma $\sigma_1$ | −1 |
| Glucocorticoid | −1 | Sodium Channel, Site 2 | 20 |
| Glutamate, Kainate | −2 | Tachykinin $NK_1$ | 22 |
| Glutamate, NMDA, Agonism | 1 | Thyroid Hormone | 6 |
| Glutamate, NMDA, Glycine | 4 | Transporter, Dopamine (DAT) | 4 |
| Glutamate, NMDA, Phancyclidine | −5 | Transporter, GABA | 11 |
| Histamine, $H_1$ | 37 | Transporter, Norepinephrine (NET) | 12 |
| Histamine, $H_2$ | 20 | Transporter, Serotonin (5-hydroxytryptamine) (SERT) | 2 |

[a]Values represent the percent inhibition of radioligand binding to designated targets at 10 $\mu$M ML352.

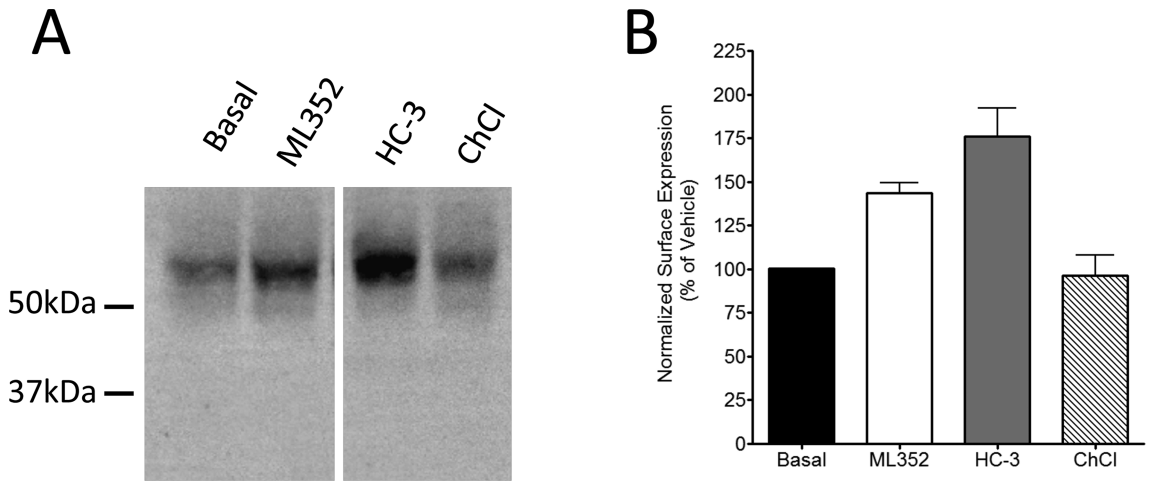


**Figure 5.** ML352 causes an increase in CHT surface expression in hCHT transfected cells. (A) Saturating concentrations, 5 $\mu$M, of ML352 or HC-3 were incubated for 15 min with wild-type (WT) hCHT transfected HEK 293 cells, followed by cell surface biotinylation and analysis of surface proteins as described in Methods. A representative western blot of surface protein levels is shown. (B) Quantitation of CHT surface expression studies. Both HC-3 and ML352 significantly elevated CHT surface protein levels (* = $P < 0.05$, Dunnett's posthoc comparison vs vehicle treated samples ($n = 4$) following a significant one-way ANOVA treatment effect ($P < 0.001$)).

(data not shown). Further studies are needed to determine the basis for these changes, for example, whether they arise from similar protein conformations or whether they derive from enhanced rates of surface delivery or recycling vs diminished


DOI: 10.1021/cn5001809
ACS Chem. Neurosci. 2015, 6, 417−427

endocytosis. Here, cells expressing the hCHT LV-AA mutant, with its significantly reduced endocytic rate, may be particularly helpful.

**ML352 Pharmacokinetics.** Lastly, we evaluated ML352 in a battery of pharmacokinetic assays (Table 2), including an assessment of intrinsic clearance ($CL_{int}$) in hepatic microsomes, allowing for the prediction of pertinent rat and human PK parameters (clearance, CL, and half-life, $t_{1/2}$). From these data, ML352 is predicted to have moderate clearance in rat ($CL_{int}$ = 95.0 mL/min/kg, $CL_{hep}$ = 40.3 mL/min/kg) and low clearance in human ($CL_{int}$ = 10.4 mL/min/kg, $CL_{hep}$ = 6.9 mL/min/kg), possessing an elevated unbound fraction ($F_u$, 0.67 in human, 0.35 in rat), as assessed via equilibrium dialysis in plasma. We also found that ML352 displayed no inhibition of four principal xenobiotic-metabolizing cytochrome P450s (3A4 (>30 $\mu$M), 2D6 (>30 $\mu$M), 2C9 (>30 $\mu$M), and 1A2 (>30 $\mu$M)). In addition to its *in vitro* pharmacodynamic profiling, the pharmacokinetic properties of ML352 were evaluated *in vivo* in male SD rats. The compound displayed plasma clearance in rats that exceeded hepatic output (CL, 107 mL/min/kg), an observation that correlated to the *in vitro* intrinsic clearance values obtained in rat hepatic microsomes ($CL_{int}$, 95 mL/min/kg); the elevated plasma clearance and high volume of distribution predicted at steady state ($V_{ss}$) resulted in a 30 min half-life for ML352. In a tissue distribution study, ML352 displayed modest brain penetration (brain $K_p$ = 0.2), reinforcing its potential for use in probing CNS components of CHT function *in vivo*. Studies are underway to further diversify the structure, with a goal of reducing clearance rates while maintaining CHT inhibitory potency, limited off-target effects, and CNS penetration.

**Table 2. Pharmacokinetic Profile of ML352**

| | | |
|---|---|---|
| MW | | 387.2 |
| cLogP | | 3.37 |
| TPSA | | 76.8 |
| *in vitro* PK parameters | human | rat |
| $CL_{int}$ (mL/min/kg) | 10.4 | 95.0 |
| $CL_{hep}$ (mL/min/kg) | 6.9 | 40.3 |
| PPB ($F_u$) | 0.67 | 0.35 |
| PBS solubility | 98.2 ± 1.1 $\mu$M | |
| P450 1A2 | >30 $\mu$M | |
| P450 2C9 | >30 $\mu$M | |
| P450 2D6 | >30 $\mu$M | |
| P450 3A4 | >30 $\mu$M | |
| *in vitro* PK parameters (Sprague–Dawley rats) | | |
| IV (1 mg/kg) | | |
| CL (mL/min/kg) | | 107 |
| $t_{1/2}$ (min) | | 33 |
| $V_{ss}$ (L/kg) | | 3.2 |
| AUC | | 150 |
| PO (2.3 mg/kg) | | |
| $C_{max}$ (ng/mL) | | 32.6 |
| $T_{max}$ (h) | | 0.25 |
| AUC (ng h/mL) | | 77.5 |
| F (%) | | 22 |
| tissue distribution (IV, 1 mg/kg, 0.25 h) | | |
| plasma (ng/mL) | | 129 |
| brain (ng/g) | | 23.4 |
| CSF (ng/g) | | 11.8 |
| $K_{p,brain}$ | | 0.2 |

In summary, we have successfully broadened the pharmacology of CHT antagonism, providing a novel tool for the study of CHT in both heterologous and native preparations and a platform for further drug development. Certainly, issues related to the potential broad physiological actions of CHT antagonism must be considered as one evaluates the potential clinical utility of CHT inhibitors, although relatively nonspecific reagents are commonly used in medical practice (e.g., amphetamines for the treatment of ADHD, clozapine for the treatment of schizophrenia). Importantly, CHT is highly regulated with respect to its contribution to cholinergic signaling due to a steady-state enrichment of the transporter on cholinergic synaptic vesicles.[34,65,66] As a consequence of its vesicular localization, CHT exhibits activity-dependent shuttling to the plasma membrane in response to presynaptic excitation. The latter property may afford CHT inhibitors a unique profile of activity-dependent, cholinergic signaling inhibition, exerting their most prominent effects under conditions of excessive ACh signaling. The noncompetitive nature of CHT inhibition by ML-352 may also provide a spectrum of properties related to *in vivo* use distinct from the actions of HC-3.

## METHODS

**Reagents and Cells.** All biochemical reagents were of research grade and, unless stated otherwise, obtained from Sigma-Aldrich (St. Louis, MO, USA). Commercially available replicates and derivatives of molecules identified as hits in our HTS screen were obtained from Ambinter (Orleans, France) as dry powders. HEK 293 and HEK 293 cells stably transfected with either the human CHT (hCHT) or mutant hCHT LV-AA (L531A, V532A) were described previously[41] and maintained according to American Type Culture Collection (ATCC, Manassas, VA, USA) guidelines using MEM Earles media containing 1× fetal bovine serum, 2 mM glutamine, 100 IU penicillin, and 100 $\mu$g/mL streptomycin (Fisher Scientific, Pittsburgh, PA, USA). All studies used cells cultured at 70–100% confluence.

**Choline-Induced Membrane Potential Assay (384-Well HTS Format).** HEK 293 cells stably expressing hCHT or hCHT LV-AA or control cells were assessed for basal and choline-induced changes in membrane depolarization as previously described[41] by plating into 384-well, black walled, clear bottom poly-D-lysine coated plates (BioCoat, BD Biosciences, San Jose, CA, USA) at 20 000 cells in 20 $\mu$L/well, dispensed using a Thermo Electron Multidrop reagent dispenser. Plated cells were grown overnight at 37 °C. The following day, the culture medium was removed, plates were washed 3× with an ELX microplate washer (Biotek, Winooski, VT, USA), and 20 $\mu$L/well of 1.67 $\mu$g/mL of the membrane potential dye (Molecular Devices, Sunnyvale, CA, USA, R8042) was added in assay buffer (Hanks balanced salt solution (HBSS), Gibco) containing 20 mM HEPES, pH 7.3, by a dispenser (Thermo). Cells were incubated for 30 min at 37 °C in an atmosphere of 95% air/5% $CO_2$ prior to addition of compounds at 2.5× their final concentration in HBSS. For control plates, a choline concentration curve ± HC-3 was prepared in assay buffer at 5× the final concentration to be assayed. Data from these experiments were used to estimate $EC_{20}$ (500 nM) and $EC_{80}$ (60 $\mu$M) concentrations for choline-induced membrane depolarization that were later used in inhibitor screening assays. Cell plates and compound plates were loaded into a Hamamatsu FDSS 6000 kinetic imaging plate reader. Baseline fluorescence signals were collected for 9 s at 0.5 Hz prior to addition of media, 5 $\mu$M HC-3, or test compounds at various concentrations, diluted from DMSO stocks. After a subsequent 2 min 16 s of recording, choline chloride at $EC_{20}$ was added (time point 2 min 25 s), followed 2.5 min later by the addition of $EC_{80}$ choline (time point 6 min), with data collected for an additional 2.5 min. Fluorescence was captured by Hamamatsu FDSS 6000 imaging software, and data were exported to Microsoft Excel for graphical and statistical analysis.

**Choline-Induced Membrane Potential Assay (96-Well FlexStation Format).** HEK 293T cells stably expressing hCHT LV-AA or


DOI: 10.1021/cn5001809
ACS Chem. Neurosci. 2015, 6, 417–427

control cells were assessed for choline-induced membrane depolarization as previously described.[41] Briefly, cells were plated into 96-well, black walled, clear bottom poly-D-lysine coated plates (BioCoat BD Biosciences). Cells were plated in 50 μL/well at 45 000 cells/well and allowed to grow for 48 h. Cells were preincubated in HBSS/HEPES 1× dye (60 μL of blue membrane potential dye, R8042 at 1.67 μg/mL, Molecular Devices, Sunnyvale, CA, USA) for 30 min at 37 °C in an atmosphere of 95% air/5% $CO_2$. Tested compounds were added at this preincubation step. Membrane potential-associated fluorescence was detected using a FlexStation (Molecular Devices) microplate fluorimeter, recording baseline (1 min) and following automated addition of choline (20 μL) to achieve 100 nM and 10 μM final concentrations in HBSS/HEPES 1× dye. Fluorescence was recorded for 2−4 min with sampling every 1.5 s. Data were analyzed by SoftMax Pro (Molecular Devices) and exported to Microsoft Excel for further evaluation.

**Neurotransmitter Transport Activity Assay (96-Well Format).** Cells were plated into poly-D-lysine coated, 96-well, white cell culture plates (Culturplate-96, PerkinElmer, Waltham, MA, USA) at 45 000 HEK293 hCHT LV-AA cells or 20 000 HEK293 hDAT, hNET, or hSERT cells in 100 μL/well and allowed to grow for 48 h at 37 °C in an atmosphere of 95% air/5% $CO_2$. Each plate was washed 3× with 100 μL of KRH using a Biotek 405 Touch microplate washer (Winooski, VT, USA). Wells were filled with 40 μL of KRH buffer with or without drugs using a multichannel pipet. Plates were incubated at 37 °C in an atmosphere of 95% air/5% $CO_2$ for 15 min for choline uptake assays and 10 min for DA, NE, and 5-HT uptake assays. Following the first incubation, an addition of 10 μL of either 100 nM or 10 μM (final concentrations) [$^3$H]-choline chloride (PerkinElmer, Waltham, MA, USA, NET109001MC, 1 mCi/mL) or 50 nM (final concentrations) [$^3$H]DA, (dihydroxyphenylethylamine,3,4-[Ring-2,5,6-$^3$H]) (PerkinElmer, NET673001MC, 1 mCi/mL), [$^3$H]NE (norepinephrine hydrochloride, DL-[7-$^3$H(N)]) (PerkinElmer, NET048001MC, 1 mCi/mL), [$^3$H]5-HT (hydroxytryptamine creatinine sulfate) (5-HT), or 5-[1,2-$^3$H(N)] (PerkinElmer, NET498001MC, 1 mCi/mL) in KRH buffer. Final concentrations of substrates solutions were made using 1% radioligand with 99% unlabeled neurotransmitter stock solution. After a 10−15 min incubation with radiolabeled substrates, each plate was washed 3× with 100 μL of KRH buffer using a Biotek (location) 405 Touch microplate washer. A volume of 100 μL of MicroScint-20 (PerkinElmer, Waltham, MA, USA) was added to wells, and uptake was quantified by scintillation spectrometry using a TopCount instrument (PerkinElmer, Waltham, MA, USA). Counts obtained from wells incubated as noted above in the presence of inhibitors of CHT (HC-3, 10 μM), DAT (cocaine, 1 μM), NET (mazindol, 1 μM), and SERT (citalopram, 1 μM) were subtracted from total uptake values to obtained specific uptake values. In saturation choline transport studies, serial dilutions from a 1−5% mix of radiolabeled and unlabeled choline was used to maintain specific activity. Choline transport velocity ($V_{max}$), half saturation concentrations ($K_m$), and antagonist $K_i$ values were determined using nonlinear curve fits in Prism 5 (GraphPad Inc., San Diego, CA, USA).

**Hemicholinium-3 (HC-3) Radioligand Binding Assays.** HEK 293 cells stably expressing CHT were plated on 150 mm sterile tissue culture dish and allowed to grow to confluence. Cells were harvested from the plates with 50 mM Tris-HCl buffer (pH 7.5) and homogenized using a Polytron (Wheaton Instruments, Millville, NJ, USA) at a speed setting of 4. Homogenates were centrifuged for 15 min at 15 000*g*. Pellets were resuspended in 10 mL of 50 mM Tris-HCl buffer (pH 7.5) and centrifuged again for 15 min at 15 000*g*. The resulting pellets were resuspended in 2 mL of Tris base buffer. Protein concentrations were determined using the BCA protein assay (Pierce, Rockford, IL, USA). Hemicholinium-3 diacetate salt, [methyl-$^3$H]-HC-3 (PerkinElmer, Waltham, MA, 120 Ci/mmol) binding assays were conducted in 50 mM TRIS-HCl buffer, 200 mM NaCl, pH 7.5, at 37 °C for 45 min. For saturation assays, serial dilutions from a 1% mix of radiolabeled and unlabeled antagonist was used to maintain specific activity. For ML352 competition binding assays, 100 μg of membranes was incubated for designated times in 10 nM [$^3$H]-HC-3 ± varying drug concentrations. Nonspecific binding in competition assays was defined in parallel incubations with 20 μM unlabeled HC-3 and subtracted from total counts to define specific HC-3 binding. Nonspecific binding in saturation binding assays was defined using membranes from non-transfected HEK 293 cells. Radioactively labeled membranes were harvested on glass fiber filters (Whatman GF/B, Brandel, Gaithersburg, MD, USA) that were pretreated with 0.3% polyethylenimine and 0.2% BSA and rinsed 4× with assay buffer (50 mM Tris-HCl, 200 mM NaCl, pH 7.5). Filters were solubilized in EcoScint H (National Diagnostics, Atlanta, GA) and allowed to shake overnight, and bound radiolabel was quantified by liquid scintillation counting (TriCarb 2900TR, PerkinElmer). HC-3 binding capacity ($B_{max}$) and affinity ($K_d$) and ML352 $K_i$ values were determined using nonlinear curve fit to a single-site inhibition model using Prism 5.

**Off-Target Screen.** ML352 was tested in the Lead Profiling Screen (Eurofin, Luxembourg), a binding assay panel of 68 G-protein coupled receptors, ion channels, and transporters, at 10 μM. The Lead Profiling Screen consists of 68 primary molecular targets, including several CNS targets recommended by the European Medicines Agency (EMEA) to evaluate drug dependence potential. For full assay details, see www.eurofinspanlabs.com.

**Animal Care and Husbandry.** All procedures with mice (C57BL/6J mice, Jackson Laboratories, Bar Harbor, ME, USA) and rats (Sprague−Dawley, Harlan, Indianapolis, IN, USA) were performed with animals at 10−20 weeks of age under an approved protocol that is reviewed annually by the Vanderbilt Institutional Animal Care and Use Committee (IACUC). Animals were housed prior to use on a 12:12 light−dark cycle with food and water provided *ad libitum*.

**Synaptosomal Transport Assays.** Male mice (C57BL/6J, Jackson Laboratories) at 8−10 weeks of age were sacrificed by rapid decapitation under urethane anesthesia, brains were removed, and brain regions were dissected on an ice-cold aluminum plate on ice. Crude synaptosomes (P2) were prepared from isolated forebrain tissue as previously described,[35] with forebrain defined as all brain tissue anterior to a coronal plane abutting the superior colliculus. Aliquots (100 μL) of crude synaptosomes (P2) were incubated with 100 μL of 100 nM radiolabeled choline, dopamine, or serotonin (materials noted above) in Kreb's bicarbonate buffer (118 mM NaCl, 4.7 mM KCl, 1.2 mM $KH_2PO_4$, 25 mM $NaHCO_3$, 1.7 mM $CaCl_2$, 10 mM glucose, 100 mM ascorbic acid) in the presence and absence of 10 μM HC-3, or other inhibitors, also as noted above, for 15 min for choline uptake assays and 10 min for all other neurotransmitters at 37 °C. Transport assays were terminated by transferring the tubes to an ice bath followed by rapid filtration over a Brandel cell harvester (Brandel Inc., Gaithersburg, MD, USA). Accumulated radioactivity was determined by scintillation spectrometry. Protein concentrations were measured using the Pierce BCA protein assay kit (Thermo Fisher Scientific Inc., Rockford, IL, USA). Specific uptake was defined with parallel incubations with specific transporter inhibitors as noted for transfected cells. Saturation kinetic parameters were determined using Prism 5 as described in cell studies.

**Metabolism and Disposition Methods.** The metabolism of ML352 was investigated *in vitro* in rat hepatic microsomes (BD Biosciences, Billerica, MA, USA) using substrate depletion methodology (% test article remaining). A potassium phosphate-buffered reaction mixture (0.1 M, pH 7.4) of test article (1 μM) and microsomes (0.5 mg/mL) was preincubated (5 min) at 37 °C prior to the addition of NADPH (1 mM). The incubations, performed in 96-well plates, were continued at 37 °C under ambient oxygenation, and aliquots (80 μL) were removed at selected time intervals (0, 3, 7, 15, 25, and 45 min). Protein was precipitated by the addition of chilled acetonitrile (160 μL), containing carbamazepine as an internal standard (50 ng/mL), and centrifuged at 3000 rpm (4 °C) for 10 min. Resulting supernatants were transferred to new 96-well plates in preparation for LC/MS/MS analysis. The *in vitro* half-life ($t_{1/2}$, min, eq 1), intrinsic clearance ($CL_{int}$, mL/min/kg, eq 2), and subsequent predicted hepatic clearance ($CL_{hep}$, mL/min/kg, eq 3) were determined employing the following equations:

$$t_{1/2} = \ln(2)/k \quad (1)$$

where $k$ represents the slope from linear regression analysis (% test article remaining)


DOI: 10.1021/cn5001809
ACS Chem. Neurosci. 2015, 6, 417−427

$$CL_{int} = (0.693/t_{1/2})(\text{rxn volume/mg of microsomes})(45\ \text{mg microsomes/g of liver})(20^{a}\ \text{g of liver/kg body weight}) \quad (2)$$

[a]scale-up factors of 20 (human) and 45 (rat)

$$CL_{hep} = \frac{Q \times CL_{int}}{Q + CL_{int}} \quad (3)$$

**Plasma Protein Binding.** Protein binding of ML352 was determined in rat plasma via equilibrium dialysis employing single-use RED plates with inserts (ThermoFisher Scientific, Rochester, NY, USA). Briefly, commercially available rat plasma (220 μL) was added to the 96-well plate containing test article (5 μL) and mixed thoroughly. Subsequently, 200 μL of the plasma−test article mixture was transferred to the *cis* chamber (red) of the RED plate, with an accompanying 350 μL of phosphate buffer (25 mM, pH 7.4) in the *trans* chamber. The RED plate was sealed and incubated for 4 h at 37 °C with shaking. At completion, 50 μL aliquots from each chamber were diluted 1:1 (50 μL) with either plasma (*cis*) or buffer (*trans*) and transferred to a new 96-well plate, at which time ice-cold acetonitrile (2 volumes), containing carbamazepine as internal standard (50 ng/mL), was added to extract the matrices. The plate was centrifuged (3000 rpm, 10 min), and supernatants were transferred to a new 96-well plate. The sealed plate was stored at −20 °C until LC/MS/MS analysis.

**Pharmacokinetics and Brain Tissue Distribution Studies in Sprague−Dawley Rats.** ML352 was formulated in 10% EtOH/50% PEG400/40% saline, as well as 0.5% methylcellulose/0.1% Tween 80, in preparation from intravenous (IV) and oral (PO) dosing, respectively. The IV dose was administered via the jugular vein to 4 dual-cannulated (carotid artery and jugular vein) adult male Sprague−Dawley rats, each weighing between 250 and 350 g (Harlan, Indianapolis, IN, USA), for a final dose of 1 mg/kg ML352; the PO dose was administered via oral gavage to 4 dual-cannulated (carotid artery and jugular vein) adult male Sprague−Dawley rats, each weighing between 250 and 350 g, for a final dose of 2.3 mg/kg dose of ML352. Whole blood collections from the IV study via the carotid artery were performed at 0.033, 0.117, 0.25, 0.5, 1, 2, 4, 7, and 24 h postdose; the PO sampling times were 0.25, 0.5, 1, 2, 3, 4, 6, 8, and 24 h postdose. Following the 24 h sample collection, rats were redosed with ML352 (1 mg/kg) followed by isoflurane treatment (0.75 min) 15 min post second dose in order to obtain blood and CNS tissue for the $K_{p,brain}$ determinations. The samples for pharmacokinetic analysis were collected into chilled, EDTA-fortified tubes and centrifuged for 10 min (3000 rcf, 4 °C), with the resulting separated plasma stored at −80 °C until LC/MS/MS bioanalysis. The samples for brain tissue distribution analysis were collected at the time of euthanization, with the whole brain being removed and thoroughly rinsed with cold phosphate-buffered saline prior to freezing on dry ice. Whole brains were weighed and diluted (3 mL) with 70:30 isopropanol/water (v/v). The mixture was subjected to mechanical homogenation employing a mini-beadbeater and 1.0 mm Zirconia/Silica Beads (BioSpec Products Inc., Bartlesville, OK, USA) followed by centrifugation (3500 rcf, 20 °C, 5 min). The liquid extraction of plasma (40 μL) and brain homogenate supernatant diluted (4×) in plasma (40 μL) was performed by conventional protein precipitation using three volumes of ice-cold acetonitrile containing an internal standard (50 nM carbamazepine). The samples were centrifuged (3500 rcf, 20 °C, 5 min), and the supernatants diluted (1:1; v/v) via transfer into a fresh 96-well plate containing deionized water for LC/MS/MS bioanalysis (*vide infra*).

**Liquid Chromatography/Mass Spectrometry Analysis.** Compounds were analyzed via electrospray ionization (ESI) on an AB Sciex API-5500 (Foster City, CA, USA) triple-quadruple linear ion trap instrument that was coupled with Shimadzu LC-20AD pumps (Columbia, MD, USA) and a Leap Technologies CTC PAL autosampler (Carrboro, NC, USA). Analytes were separated by gradient elution using a Fortis C18 2.1 × 50 mm, 3.5 μm column (Fortis Technologies Ltd., Cheshire, UK) thermostated at 40 °C. HPLC mobile phase A was 0.1% $NH_4OH$ (pH unadjusted), and mobile phase B was acetonitrile. The gradient started at 30% B after a 0.2 min hold and was linearly increased to 90% B over 0.8 min, held at 90% B for 0.5 min, and returned to 30% B in 0.1 min followed by a re-equilibration (0.9 min). The total run time was 2.5 min, and the HPLC flow rate was 0.5 mL/min. The source temperature was set at 500 °C, and mass spectral analyses were performed using multiple reaction monitoring (MRM) utilizing a turbo-ionspray source in positive ionization mode (5.0 kV spray voltage). LC/MS/MS analysis was performed employing a TSQ Quantum$^{ULTRA}$ that was coupled to a ThermoSurveyor LC system (Thermoelectron Corp., San Jose, CA, USA) and a Leap Technologies CTC PAL autosampler (Carrboro, NC, USA). Chromatographic separation of analytes was achieved with an Acquity BEH C18 2.1 × 50 mm, 1.7 μm column (Waters, Taunton, MA, USA).

**Evaluation of CHT Surface Expression.** Cell surface biotinylation assays to evaluate impact of selected compounds on CHT surface expression were performed as previously described[41] using EZ-Link Sulfo-NHS-SS-Biotin (Pierce, Rockford, IL, USA). Following treatments of hCHT transfected HEK 293 cells with or without choline (10 μM), HC-3 (5 μM), or ML352 for 15 min, cells were biotinylated on ice for 1 h, followed by a 30 min incubation with 1× PBS with calcium, magnesium, and 100 mM glycine. Cells were extracted with 500 μL of RIPA buffer (10 mM Tris-HCl, 100 mM NaCl, 1 mM EDTA, 0.1% SDS, 1% Triton-X 100, 10 g/L deoxycholate), and biotinylated proteins were isolated using Ultralink Avidin (Pierce, Rockford, IL, USA), eluted in Laemmli buffer,[67,68] resolved by 10% acrylamide SDS-PAGE, and blotted to PVDF membrane (Millipore, Darmstadt, Germany). PVDF membranes were blocked in PBST + 5% nonfat drymilk (PBST-M) for 1 h and then probed with 10 mL of polyclonal rabbit (1:500 to 1:1000) anti-CHT antibody[34] for CHT overnight at 4 °C. Blots were rinsed 3× for 5 min in PBST and incubated in HRP-conjugated secondary antibody (goat anti-rabbit, 1:5000 in PBS-TM, Jackson Immunoresearch, West Grove, PA, USA) for 1 h at room temperature. Blots were rinsed 3× for 5 min in PBST and developed by chemiluminescence (Western Lightning Enhanced Chemiluminescence kit, PerkinElmer, Waltham, MA, USA). Blots developed using a LAS4000 Chemiluminescent and GFP CCD Imager (GE Healthcare, Buckinghamshire, England). ImageQuant software (GE Healthcare, Buckinghamshire, England) was used to determine the band densities. In order to compensate for interexperiment variability, CHT bands were normalized to CHT protein detected in total protein extracts. Cumulative were analyzed by a one-way ANOVA with Dunnett's planned comparisons of drug vs vehicle, with $P < 0.05$ taken as being significant (Prism 5.0).

## AUTHOR INFORMATION


### Corresponding Author

*Tel: 615-936-1700. E-mail: randy.blakely@vanderbilt.edu.


### Author Contributions

Corey R. Hopkins, Randy D. Blakely, Jane Wright, Elizabeth A. Ennis, Owen B. McManus, Zhinong Lin, Xiaofang Huang, Meng Wu, and Min Li participated in the establishment and execution of the high-throughput screen at the Johns Hopkins Ion Channel Center. Elizabeth Ennis completed the majority of the compound screening, cell, synaptosomal, specificity, and biotinylation assays. Jane Wright and Cassandra L. Retzlaff aided in the completion of the synaptosomal uptake assays, and the cell surface biotinylation assays, respectively. J. Scott Daniels and Craig W. Lindsley directed the drug metabolism and pharmacokinetic experiments. All of the aforementioned authors participated in the discussions that guided the work at various stages. Elizabeth A. Ennis and Randy D. Blakely wrote the text for this article with input on manuscript revisions provided by all of the authors.


### Funding

This research was supported by CTSA award UL1TR000445 from the National Center for Advancing Translational Sciences (E.A.E.), and NIH awards GM07628 (E.A.E.), MH073159




DOI: 10.1021/cn5001809
*ACS Chem. Neurosci.* 2015, 6, 417−427

(R.D.B.), NIH/MLPCN grant U54 MH084659 (C.W.L.), and a Zenith Award from the Alzheimer's Foundation (R.D.B.).

### Notes

The authors declare no competing financial interest.

## ■ ACKNOWLEDGMENTS

The authors thank Alicia M. Ruggiero for initial efforts to establish the screen, Angela Steele, Qiao Han, and Chris Svitek for general laboratory assistance, and Ryan Morrison and Frank Byers for technical assistance associated with the pharmacokinetic experiments.

## ■ REFERENCES

(1) Kandel, E. R. (2013) *Principles of Neuroscience*, 5th ed., McGraw-Hill, New York.
(2) Mark, G. P., Shabani, S., Dobbs, L. K., and Hansen, S. T. (2011) Cholinergic modulation of mesolimbic dopamine function and reward. *Physiol. Behav. 104*, 76−81.
(3) Hasselmo, M. E., and Sarter, M. (2011) Modes and models of forebrain cholinergic neuromodulation of cognition. *Neuropsychopharmacology 36*, 52−73.
(4) Doody, R. S. (2003) Current treatments for Alzheimer's disease: cholinesterase inhibitors. *J. Clin. Psychiatry 64*, 11−17.
(5) Manganelli, F., Vitale, C., Santangelo, G., Pisciotta, C., Iodice, R., Cozzolino, A., Dubbioso, R., Picillo, M., Barone, P., and Santoro, L. (2009) Functional involvement of central cholinergic circuits and visual hallucinations in Parkinson's disease. *Brain 132*, 2350−2355.
(6) Sciamanna, G., Tassone, A., Mandolesi, G., Puglisi, F., Ponterio, G., Martella, G., Madeo, G., Bernardi, G., Standaert, D. G., Bonsi, P., and Pisani, A. (2012) Cholinergic dysfunction alters synaptic integration between thalamostriatal and corticostriatal inputs in DYT1 dystonia. *J. Neurosci. 32*, 11991−12004.
(7) Sciamanna, G., Hollis, R., Ball, C., Martella, G., Tassone, A., Marshall, A., Parsons, D., Li, X., Yokoi, F., Zhang, L., Li, Y., Pisani, A., and Standaert, D. G. (2012) Cholinergic dysregulation produced by selective inactivation of the dystonia-associated protein torsinA. *Neurobiol. Dis. 47*, 416−427.
(8) Pisani, A., Bernardi, G., Ding, J., and Surmeier, D. J. (2007) Re-emergence of striatal cholinergic interneurons in movement disorders. *Trends Neurosci. 30*, 545−553.
(9) Higley, M. J., and Picciotto, M. R. (2014) Neuromodulation by acetylcholine: examples from schizophrenia and depression. *Curr. Opin. Neurobiol. 29C*, 88−95.
(10) Williams, M. J., and Adinoff, B. (2008) The role of acetylcholine in cocaine addiction. *Neuropsychopharmacology 33*, 1779−1797.
(11) Wilkinson, D. G., Francis, P. T., Schwam, E., and Payne-Parrish, J. (2004) Cholinesterase inhibitors used in the treatment of Alzheimer's disease: the relationship between pharmacological effects and clinical efficacy. *Drugs Aging 21*, 453−478.
(12) Koegelenberg, C. F., Noor, F., Bateman, E. D., van Zyl-Smit, R. N., Bruning, A., O'Brien, J. A., Smith, C., Abdool-Gaffar, M. S., Emanuel, S., Esterhuizen, T. M., and Irusen, E. M. (2014) Efficacy of varenicline combined with nicotine replacement therapy vs varenicline alone for smoking cessation: a randomized clinical trial. *J. Am. Med. Assoc. 312*, 155−161.
(13) Jankovic, J. (2013) Medical treatment of dystonia. *Mov. Disord. 28*, 1001−1012.
(14) Simon, J. R., Atweh, S., and Kuhar, M. J. (1976) Sodium-dependent high affinity choline uptake: a regulatory step in the synthesis of acetylcholine. *J. Neurochem. 26*, 909−922.
(15) Okuda, T., Haga, T., Kanai, Y., Endou, H., Ishihara, T., and Katsura, I. (2000) Identification and characterization of the high-affinity choline transporter. *Nat. Neurosci. 3*, 120−125.
(16) Apparsundaram, S., Ferguson, S. M., George, A. L., Jr., and Blakely, R. D. (2000) Molecular cloning of a human, hemicholinium-3-sensitive choline transporter. *Biochem. Biophys. Res. Commun. 276*, 862−867.
(17) Apparsundaram, S., Ferguson, S. M., and Blakely, R. D. (2001) Molecular cloning and characterization of a murine hemicholinium-3-sensitive choline transporter. *Biochem. Soc. Trans. 29*, 711−716.
(18) Haga, T. (2014) Molecular properties of the high-affinity choline transporter CHT1. *J. Biochem. 156*, 181−194.
(19) Bazalakova, M. H., and Blakely, R. D. (2006) The high-affinity choline transporter: a critical protein for sustaining cholinergic signaling as revealed in studies of genetically altered mice. *Handb. Exp. Pharmacol.*, 525−544.
(20) Ferguson, S. M., Bazalakova, M., Savchenko, V., Tapia, J. C., Wright, J., and Blakely, R. D. (2004) Lethal impairment of cholinergic neurotransmission in hemicholinium-3-sensitive choline transporter knockout mice. *Proc. Natl. Acad. Sci. U.S.A. 101*, 8762−8767.
(21) English, B. A., Appalsamy, M., Diedrich, A., Ruggiero, A. M., Lund, D., Wright, J., Keller, N. R., Louderback, K. M., Robertson, D., and Blakely, R. D. (2010) Tachycardia, reduced vagal capacity, and age-dependent ventricular dysfunction arising from diminished expression of the presynaptic choline transporter. *Am. J. Physiol.: Heart Circ. Physiol. 299*, H799−810.
(22) Holmstrand, E. C., Lund, D., Cherian, A. K., Wright, J., Martin, R. F., Ennis, E. A., Stanwood, G. D., Sarter, M., and Blakely, R. D. (2013) Transgenic overexpression of the presynaptic choline transporter elevates acetylcholine levels and augments motor endurance. *Neurochem. Int. 73*, 217−228.
(23) Lund, D., Ruggiero, A. M., Ferguson, S. M., Wright, J., English, B. A., Reisz, P. A., Whitaker, S. M., Peltier, A. C., and Blakely, R. D. (2010) Motor neuron-specific overexpression of the presynaptic choline transporter: impact on motor endurance and evoked muscle activity. *Neuroscience 171*, 1041−1053.
(24) Parikh, V., St. Peters, M., Blakely, R. D., and Sarter, M. (2013) The presynaptic choline transporter imposes limits on sustained cortical acetylcholine release and attention. *J. Neurosci. 33*, 2326−2337.
(25) Zurkovsky, L., Bychkov, E., Tsakem, E. L., Siedlecki, C., Blakely, R. D., and Gurevich, E. V. (2013) Cognitive effects of dopamine depletion in the context of diminished acetylcholine signaling capacity in mice. *Dis. Models & Mech. 6*, 171−183.
(26) Dong, Y., Dani, J. A., and Blakely, R. D. (2013) Choline transporter hemizygosity results in diminished basal extracellular dopamine levels in nucleus accumbens and blunts dopamine elevations following cocaine or nicotine. *Biochem. Pharmacol. 86*, 1084−1088.
(27) Bater, K., and Blakely, R. D., in preparation.
(28) Barwick, K. E., Wright, J., Al-Turki, S., McEntagart, M. M., Nair, A., Chioza, B., Al-Memar, A., Modarres, H., Reilly, M. M., Dick, K. J., Ruggiero, A. M., Blakely, R. D., Hurles, M. E., and Crosby, A. H. (2012) Defective presynaptic choline transport underlies hereditary motor neuropathy. *Am. J. Hum. Genet. 91*, 1103−1107.
(29) Berry, A. S., Demeter, E., Sabhapathy, S., English, B. A., Blakely, R. D., Sarter, M., and Lustig, C. (2014) Disposed to distraction: genetic variation in the cholinergic system influences distractibility but not time-on-task effects. *J. Cogn. Neurosci.*, 1−11.
(30) English, B. A., Hahn, M. K., Gizer, I. R., Mazei-Robison, M., Steele, A., Kurnik, D. M., Stein, M. A., Waldman, I. D., and Blakely, R. D. (2009) Choline transporter gene variation is associated with attention-deficit hyperactivity disorder. *J. Neurodev. Disord. 1*, 252−263.
(31) Hahn, M. K., Blackford, J. U., Haman, K., Mazei-Robison, M., English, B. A., Prasad, H. C., Steele, A., Hazelwood, L., Fentress, H. M., Myers, R., Blakely, R. D., Sanders-Bush, E., and Shelton, R. (2008) Multivariate permutation analysis associates multiple polymorphisms with subphenotypes of major depression. *Genes, Brain Behav. 7*, 487−495.
(32) Ferguson, S. M., and Blakely, R. D. (2004) The choline transporter resurfaces: new roles for synaptic vesicles? *Mol. Interventions 4*, 22−37.
(33) Sarter, M., and Parikh, V. (2005) Choline transporters, cholinergic transmission and cognition. *Nat. Rev. Neurosci. 6*, 48−56.
(34) Ferguson, S. M., Savchenko, V., Apparsundaram, S., Zwick, M., Wright, J., Heilman, C. J., Yi, H., Levey, A. I., and Blakely, R. D. (2003) Vesicular localization and activity-dependent trafficking of presynaptic choline transporters. *J. Neurosci. 23*, 9697−9709.


DOI: 10.1021/cn5001809
*ACS Chem. Neurosci.* 2015, 6, 417−427

(35) Apparsundaram, S., Martinez, V., Parikh, V., Kozak, R., and Sarter, M. (2005) Increased capacity and density of choline transporters situated in synaptic membranes of the right medial prefrontal cortex of attentional task-performing rats. *J. Neurosci. 25*, 3851−3856.
(36) Vickroy, T. W., Roeske, W. R., Gehlert, D. R., Wamsley, J. K., and Yamamura, H. I. (1985) Quantitative light microscopic autoradiography of [$^3$H]hemicholinium-3 binding sites in the rat central nervous system: a novel biochemical marker for mapping the distribution of cholinergic nerve terminals. *Brain Res. 329*, 368−373.
(37) Vickroy, T. W., Roeske, W. R., and Yamamura, H. I. (1984) Sodium-dependent high-affinity binding of [$^3$H]hemicholinium-3 in the rat brain: a potentially selective marker for presynaptic cholinergic sites. *Life Sci. 35*, 2335−2343.
(38) Mulder, A. H., Yamamura, H. I., Kuhar, M. J., and Snyder, S. H. (1974) Release of acetylcholine from hippocampal slices by potassium depolarization: dependence on high affinity choline uptake. *Brain Res. 70*, 372−376.
(39) Schueler, F. W. (1955) A new group of respiratory paralyzants. I. The "hemicholiniums". *J. Pharmacol. Exp. Ther. 115*, 127−143.
(40) Schueler, F. W. (1960) The mechanism of action of the hemicholiniums. *Int. Rev. Neurobiol. 2*, 77−97.
(41) Ruggiero, A. M., Wright, J., Ferguson, S. M., Lewis, M., Emerson, K. S., Iwamoto, H., Ivy, M. T., Holmstrand, E. C., Ennis, E. A., Weaver, C. D., and Blakely, R. D. (2012) Nonoisotopic assay for the presynaptic choline transporter reveals capacity for allosteric modulation of choline uptake. *ACS Chem. Neurosci. 3*, 767−781.
(42) Iwamoto, H., Blakely, R. D., and De Felice, L. J. (2006) $Na^+$, $Cl^-$, and pH dependence of the human choline transporter (hCHT) in Xenopus oocytes: the proton inactivation hypothesis of hCHT in synaptic vesicles. *J. Neurosci. 26*, 9851−9859.
(43) Birks, R. I., and Macintosh, F. C. (1957) Acetylcholine metabolism at nerve-endings. *Br. Med. Bull. 13*, 157−161.
(44) Collier, B., and Katz, H. S. (1974) Acetylcholine synthesis from recaptured choline by a sympathetic ganglion. *J. Physiol. 238*, 639−655.
(45) Ramirez-Castaneda, J., and Jankovic, J. (2013) Long-term efficacy and safety of botulinum toxin injections in dystonia. *Toxins 5*, 249−266.
(46) Mineur, Y. S., Obayemi, A., Wigestrand, M. B., Fote, G. M., Calarco, C. A., Li, A. M., and Picciotto, M. R. (2013) Cholinergic signaling in the hippocampus regulates social stress resilience and anxiety- and depression-like behavior. *Proc. Natl. Acad. Sci. U.S.A. 110*, 3573−3578.
(47) Picciotto, M. R., Higley, M. J., and Mineur, Y. S. (2012) Acetylcholine as a neuromodulator: cholinergic signaling shapes nervous system function and behavior. *Neuron 76*, 116−129.
(48) Drevets, W. C., Zarate, C. A., Jr., and Furey, M. L. (2013) Antidepressant effects of the muscarinic cholinergic receptor antagonist scopolamine: a review. *Biol. Psychiatry 73*, 1156−1163.
(49) Voleti, B., Navarria, A., Liu, R. J., Banasr, M., Li, N., Terwilliger, R., Sanacora, G., Eid, T., Aghajanian, G., and Duman, R. S. (2013) Scopolamine rapidly increases mammalian target of rapamycin complex 1 signaling, synaptogenesis, and antidepressant behavioral responses. *Biol. Psychiatry 74*, 742−749.
(50) Crooks, P. A., Ayers, J. T., Xu, R., Sumithran, S. P., Grinevich, V. P., Wilkins, L. H., Deaciuc, A. G., Allen, D. D., and Dwoskin, L. P. (2004) Development of subtype-selective ligands as antagonists at nicotinic receptors mediating nicotine-evoked dopamine release. *Bioorg. Med. Chem. Lett. 14*, 1869−1874.
(51) Shinohara, F., Kihara, Y., Ide, S., Minami, M., and Kaneda, K. (2014) Critical role of cholinergic transmission from the laterodorsal tegmental nucleus to the ventral tegmental area in cocaine-induced place preference. *Neuropharmacology 79*, 573−579.
(52) Haga, T., and Noda, H. (1973) Choline uptake systems of rat brain synaptosomes. *Biochim. Biophys. Acta 291*, 564−575.
(53) Happe, H. K., and Murrin, L. C. (1993) High-affinity choline transport sites: use of [$^3$H]hemicholinium-3 as a quantitative marker. *J. Neurochem. 60*, 1191−1201.
(54) Happe, H. K., and Murrin, L. C. (1992) Development of high-affinity choline transport sites in rat forebrain: a quantitative autoradiography study with [$^3$H]hemicholinium-3. *J. Comp. Neurol. 321*, 591−611.
(55) Parikh, V., Pomerleau, F., Huettl, P., Gerhardt, G. A., Sarter, M., and Bruno, J. P. (2004) Rapid assessment of *in vivo* cholinergic transmission by amperometric detection of changes in extracellular choline levels. *Eur. J. Neurosci. 20*, 1545−1554.
(56) Bonsi, P., Martella, G., Cuomo, D., Platania, P., Sciamanna, G., Bernardi, G., Wess, J., and Pisani, A. (2008) Loss of muscarinic autoreceptor function impairs long-term depression but not long-term potentiation in the striatum. *J. Neurosci. 28*, 6258−6263.
(57) Michel, V., Yuan, Z., Ramsubir, S., and Bakovic, M. (2006) Choline transport for phospholipid synthesis. *Exp. Biol. Med. 231*, 490−504.
(58) Ansell, G. B., and Spanner, S. G. (1974) The inhibition of brain choline kinase by hemicholinium-3. *J. Neurochem. 22*, 1153−1155.
(59) Chatterjee, T. K., Cannon, J. G., and Bhatnagar, R. K. (1987) Characteristics of [3H]hemicholinium-3 binding to rat striatal membranes: evidence for negative cooperative site−site interactions. *J. Neurochem. 49*, 1191−1201.
(60) Zheng, Q. H., Gao, M., Mock, B. H., Wang, S., Hara, T., Nazih, R., Miller, M. A., Receveur, T. J., Lopshire, J. C., Groh, W. J., Zipes, D. P., Hutchins, G. D., and DeGrado, T. R. (2007) Synthesis and biodistribution of new radiolabeled high-affinity choline transporter inhibitors [$^{11}$C]hemicholinium-3 and [$^{18}$F]hemicholinium-3. *Bioorg. Med. Chem. Lett. 17*, 2220−2224.
(61) Sandberg, K., and Coyle, J. T. (1985) Characterization of [$^3$H]hemicholinium-3 binding associated with neuronal choline uptake sites in rat brain membranes. *Brain Res. 348*, 321−330.
(62) Manaker, S., Wieczorek, C. M., and Rainbow, T. C. (1986) Identification of sodium-dependent, high-affinity choline uptake sites in rat brain with [$^3$H]hemicholinium-3. *J. Neurochem. 46*, 483−488.
(63) Giboureau, N., Som, I. M., Boucher-Arnold, A., Guilloteau, D., and Kassiou, M. (2010) PET radioligands for the vesicular acetylcholine transporter (VAChT). *Curr. Top. Med. Chem. 10*, 1569−1583.
(64) Okuda, T., Konishi, A., Misawa, H., and Haga, T. (2011) Substrate-induced internalization of the high-affinity choline transporter. *J. Neurosci. 31*, 14989−14997.
(65) Ferguson, S. M., and Blakely, R. D. (2004) The choline transporter resurfaces: new roles for synaptic vesicles? *Mol. Interventions 4*, 22−37.
(66) Nakata, K., Okuda, T., and Misawa, H. (2004) Ultrastructural localization of high-affinity choline transporter in the rat neuromuscular junction: enrichment on synaptic vesicles. *Synapse 53*, 53−56.
(67) Black, S. A., Ribeiro, F. M., Ferguson, S. S., and Rylett, R. J. (2010) Rapid, transient effects of the protein kinase C activator phorbol 12-myristate 13-acetate on activity and trafficking of the rat high-affinity choline transporter. *Neuroscience 167*, 765−773.
(68) Gates, J., Jr., Ferguson, S. M., Blakely, R. D., and Apparsundaram, S. (2004) Regulation of choline transporter surface expression and phosphorylation by protein kinase C and protein phosphatase 1/2A. *J. Pharmacol. Exp. Ther. 310*, 536−545.


DOI: 10.1021/cn5001809
*ACS Chem. Neurosci.* 2015, 6, 417−427